DALTON
FULL PAPER

Structures and photoluminescence of dinuclear platinum(II) and palladium(II) complexes with bridging thiolates and 2,2′-bipyridine or 2,2′:6′,2″-terpyridine ligands

Biing-Chiau Tzeng,[a] Wen-Fu Fu,[a] Chi-Ming Che,*[a] Hsiu-Yi Chao,[a] Kung-Kai Cheung[a] and Shie-Ming Peng[b]

[a] *Department of Chemistry, The University of Hong Kong, Pokfulam Road, Hong Kong*
[b] *Department of Chemistry, National Taiwan University, Taipei, Taiwan*

Received 27th November 1998, Accepted 8th January 1999

A series of mononuclear and dinuclear platinum(II) thiolates with 2,2′-bipyridine (bpy) and 2,2′:6′,2″-terpyridine (terpy) ligands having emissive LLCT (ligand-to-ligand charge-transfer) excited states were prepared and characterized by X-ray diffraction analyses. The $[M_2(dtbpy)_2(NS)_2][ClO_4]_2$ (M = Pt or Pd; dtbpy = 4,4′-di-*tert*-butyl-2,2′-bipyridine, NS^- = pyridine-2-thiolate) complexes are isostructural to each other with intramolecular Pt · · · Pt and Pd · · · Pd distances being 2.917(2) and 2.891(4) Å, respectively. Assignment of LLCT absorption bands for the platinum(II) complexes was based on the shift in absorption energy with the substituents on the diimine and thiolate ligands. In the solid state or in solution at room temperature the platinum(II) complexes show photoluminescence with λ_{max} ranging from 603 to 710 nm. The $Pt^{II} \cdots Pt^{II}$ and/or ligand–ligand interactions are not primarily responsible for the emissions of the dinuclear platinum(II) thiolates which have intramolecular metal–metal separations greater than 2.9 Å.

Introduction

Recent studies have revealed new classes of platinum(II) diimine complexes, which display emissive and long-lived excited states in solution at room temperature.[1–6] A notable excited state of these complexes arises from MMLCT[2,3] (metal–metal to ligand charge transfer) transition, $d_{\sigma^*}(Pt–Pt) \longrightarrow \pi^*(diimine)$ (d_{σ^*}, antisymmetric combination of nd_{z^2} orbitals), and this occurs when two platinum(II) diimine moieties are in close proximity to allow metal–metal and/or ligand–ligand interactions. In previous works the solid state emissions of stacking platinum(II) diimine solids[2] and excimeric emissions of cyclometallated platinum(II)[4a,b] and $[Pt(diimine)(CN)_2]$[4c,5b] complexes recorded in solutions were attributed to MMLCT excited states. Interestingly, there has been no report on excimeric emission from platinum(II) thiolates of aromatic diimines, despite the rich photoluminescence of this class of compounds.[5a,6] It is likely that the soft thiolate ligand would render the S→diimine (π*) charge-transfer transition at an energy lower than that of the MMLCT one (Scheme 1).

The LLCT [ligand-to-ligand charge transfer, here, $RS^-(p_\pi) \rightarrow$ diimine(π*)] excited states had previously been noted in some zinc(II)[7] and platinum(II)[5a,6] complexes containing both N-heterocyclic (diimine) and aromatic thiolate (dithiolate) ligands. Crosby and co-workers[7] introduced this concept to rationalize the visible absorption and low-energy emission spectra of some zinc(II) thiolates containing phen (1,10-phenanthroline) ligand. In general, both electron-donating substituents on the thiolate and electron-withdrawing substituents on the diimine ligand would lower the LLCT transition energy.

The first platinum(II) complex exhibiting LLCT emission was reported by Vogler and Kunkely.[5a] These workers recorded the absorption spectrum of $[Pt(bpy)(MeC_6H_3S_2\text{-}3,4)]$ (bpy = 2,2′-bipyridine) which shows an intense low-energy absorption with λ_{max} at 558 nm in ethanol and 610 nm in chloroform. This complex emits at 654 nm in a 77 K ethanol glass. The emission was assigned to the LLCT excitation. In the literature,[5a,b] the spectroscopic and photophysical studies on LLCT transitions of Pt^{II} dealt with mononuclear species. In this work, the spectroscopic properties and crystal structures of a series of mononuclear and dinuclear platinum(II) complexes containing bridging thiolate ligands are presented. The objective was to employ discrete dinuclear platinum(II) complexes as models to probe the spectroscopic properties arising from interactions among mononuclear platinum(II) thiolate complexes containing aromatic diimines in the ground and/or excited states.

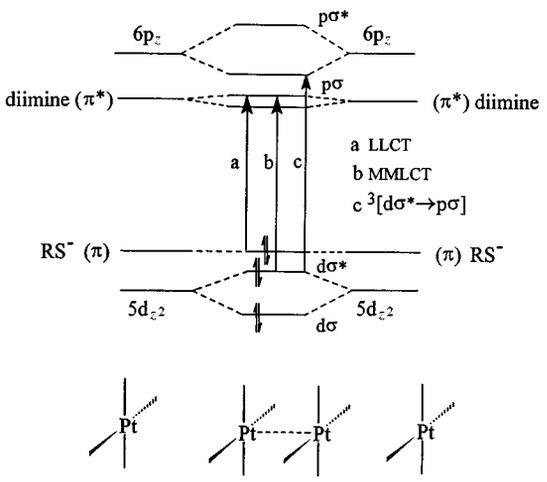

Scheme 1 Qualitative molecular orbital interaction diagram for Pt^{II}_2 complexes and the relative energy between LLCT, MMLCT and $^3[d_{\sigma^*} \longrightarrow p_\sigma]$ states.

Experimental

Materials

Pyridine-2-thiol (HNS), pyrimidine-2-thiol (HNN′S), quinoline-2-thiol (HQNS), dithiouracil (H_2SNS), 2,2′-bipyridine and 2,2′:6′,2″-terpyridine (terpy) were purchased from Aldrich Chemicals, K_2PtCl_4 from Strem Chemicals. 4,4′-Di-*tert*-butyl-2,2′-bipyridine (dtbpy),[8] [Pt(terpy)Cl]Cl,[9] $[Pt(bpy)Cl_2]$,[10] [Pt-

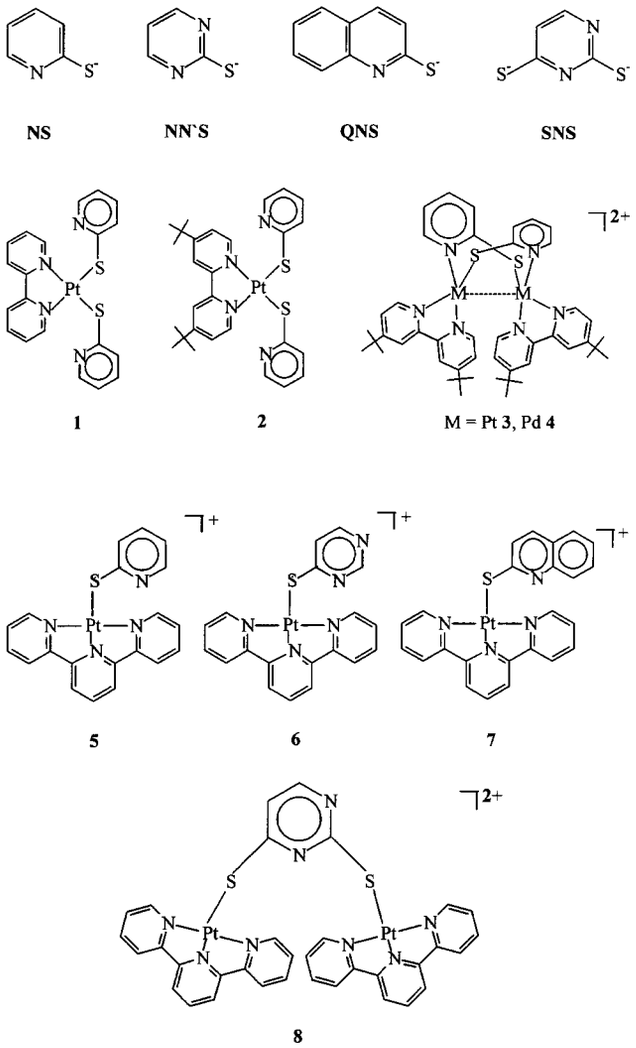

(dtbpy)Cl_2][10] and [Pd(dtbpy)Cl_2][10] were prepared according to literature methods. All solvents (Analytical grade) for synthesis were used without further purification. Solvents for photophysical studies were purified by literature methods. All operations were carried out under a nitrogen atmosphere.

Synthesis

[Pt(bpy)(NS)$_2$] 1. Stirring a mixture of [Pt(bpy)Cl_2] (1 mmol, 422 mg) and NaNS [2 mmol, 266 mg, obtained from HNS (2 mmol, 222 mg) and NaOMe (2.2 mmol, 122 mg) in MeOH (25 ml)] in MeOH (50 ml) at 50 °C for 30 min gave a red-brown solid. This was filtered off and the crude product recrystallized from CH_2Cl_2–n-hexane to give [Pt(bpy)(NS)$_2$] (yield 80%) (Found: C, 42.21; H, 3.02; N, 9.52. Calc. for $C_{20}H_{16}N_4PtS_2$: C, 42.03; H, 2.82; N, 9.80%). FAB: [Pt(bpy)(NS)$_2$], *m*/*z* = 572, 65%.

[Pt(dtbpy)(NS)$_2$] 2. The method was similar to that for the preparation of [Pt(bpy)(NS)$_2$], using [Pt(dtbpy)Cl_2] instead of [Pt(bpy)Cl_2], which gave [Pt(dtbpy)(NS)$_2$] (yield 60%) (Found: C, 49.01; H, 4.42; N, 8.02. Calc. for $C_{28}H_{32}N_4PtS_2$: C, 49.18; H, 4.72; N, 8.19%). FAB: [Pt(dtbpy)(NS)$_2$], *m*/*z* = 683, 50%.

[{Pt(dtbpy)(NS)}$_2$][ClO$_4$]$_2$ 3. A clear red-orange solution was obtained by refluxing equimolar amounts of [Pt(dtbpy)Cl_2] (1 mmol, 534 mg) and NaNS (1 mmol, 133 mg) in MeOH (50 ml) for 4 h. Upon the addition of $LiClO_4$ an red-orange solid was obtained and recrystallized by diffusion of Et_2O into a CH_2Cl_2–MeOH solution (yield 65%) (Found: C, 42.29; H, 4.12; N, 6.02. Calc. for $C_{46}H_{56}Cl_2N_6O_8Pt_2S_2{\cdot}CH_3OH$: C, 41.90; H, 4.45; N, 6.24%) FAB: [{Pt(dtbpy)(NS)}$_2$]$^{2+}$, *m*/*z* = 573, 100; [{Pt(dtbpy)(NS)}$_2$(ClO_4)]$^+$, *m*/*z* = 1246, 40%.

[{Pd(dtbpy)(NS)}$_2$][ClO$_4$]$_2$ 4. The preparation was similar to that for the platinum(II) analogue using [Pd(dtbpy)Cl_2] instead of [Pt(dtbpy)Cl_2] (yield, 85%) (Found: C, 48.31; H, 5.22; N, 7.02. Calc. for $C_{46}H_{56}Cl_2N_6O_8Pd_2S_2{\cdot}CH_3OH$: C, 48.25; H, 5.13; N, 7.19%). FAB: [{Pd(dtbpy)(NS)}$_2$]$^{2+}$, *m*/*z* = 485, 100%.

[Pt(terpy)(NS)]ClO$_4$ 5. A clear red-brown solution was obtained by refluxing equimolar amounts of [Pt(terpy)Cl_2] (1 mmol, 499 mg) and NaNS (1 mmol, 133 mg) in MeOH (50 ml) for 8 h. Upon the addition of $LiClO_4$ a red-brown solid was obtained and recrystallized by diffusion of Et_2O into a CH_3CN solution (yield 75%) (Found: C, 37.31; H, 2.22; N, 9.02. Calc. for $C_{20}H_{15}ClN_4O_4PtS$: C, 37.61; H, 2.37; N, 8.78%). FAB: [Pt(terpy)(NS)]$^+$, *m*/*z* = 538, 100%.

[Pt(terpy)(NN′S)]ClO$_4$ 6. The preparation was similar to that for complex **5** except NaNN′S was used instead of NaNS. Upon the addition of $LiClO_4$ a red-brown solid was obtained and recrystallized by diffusion of Et_2O into a CH_3CN solution (yield 80%) (Found: C, 35.51; H, 2.32; N, 10.78. Calc. for $C_{19}H_{14}ClN_5O_4PtS$: C, 35.72; H, 2.21; N, 10.96%). FAB: [Pt(terpy)(NN′S)]$^+$, *m*/*z* = 539, 45%.

[Pt(terpy)(QNS)]ClO$_4$ 7. The preparation was also similar to that for complex **5**, except NaQNS was used instead of NaNS. Upon addition of $LiClO_4$ a red-brown solid was obtained and recrystallized by diffusion of Et_2O into a CH_3CN solution (yield 65%) (Found: C, 41.56; H, 2.19; N, 7.78. Calc. for $C_{24}H_{17}ClN_4O_4PtS$: C, 41.86; H, 2.47; N, 8.14%). FAB: [Pt(terpy)(QNS)]$^+$, *m*/*z* = 588, 100%.

[{Pt(terpy)}$_2$SNS][ClO$_4$]$_2$ 8. A clear red-brown solution was obtained by refluxing 2 equivalents of [Pt(terpy)Cl_2] (1 mmol, 499 mg) and 1 equivalent of Na_2SNS (0.5 mmol, 94 mg, preparation similar to NaNS) in MeOH (50 ml) for 12 h. Upon the addition of $LiClO_4$ a red-brown solid was obtained and recrystallized by diffusion of Et_2O into a CH_3CN solution (yield 60%) (Found: C, 34.60; H, 2.22; N, 9.02. Calc. for $C_{34}H_{24}Cl_2N_8O_8Pt_2S_2$: C, 34.09; H, 2.02; N, 9.35%). FAB: [{Pt(terpy)}$_2$SNS]$^{2+}$, *m*/*z* = 499, 80%.

Physical measurements and instrumentation

The UV/VIS spectra were recorded on a Perkin-Elmer Lambda 19 spectrophotometer and steady state emission spectra on a SPEX Fluorolog-2 spectrophotometer. Room temperature solid state emission spectra were recorded with the solid samples contained in a 5 mm diameter quartz tube. Measurements of low temperature (77 K) emission spectra were similar to the room temperature ones except that the quartz tubes were placed in a liquid nitrogen dewar flask equipped with quartz windows. Emission lifetime measurements were performed with a Quanta Ray DCR-3 Nd-YAG laser (pulse output 355 nm, 8 ns). The decay signal was recorded by a R928 PMT (Hamamatsu), which was connected to a Tektronix 2430 digital oscilloscope. Solutions for photophysical experiments were degassed by at least four freeze–pump–thaw cycles. Elemental analyses of the compounds were performed by Butterworth Laboratories.

X-Ray crystallography

Complexes **1**, **3**–**6**, and **8** were characterized by X-ray crystallography. The intensity data were collected on a Enraf-Nonius CAD4 diffractometer with graphite-monochromated Mo-Kα radiation (λ = 0.7107 Å) for **1**, **5** and **6**; and with graphite-monochromated Cu-Kα radiation (λ = 1.5418 Å) for **3** and **4** at

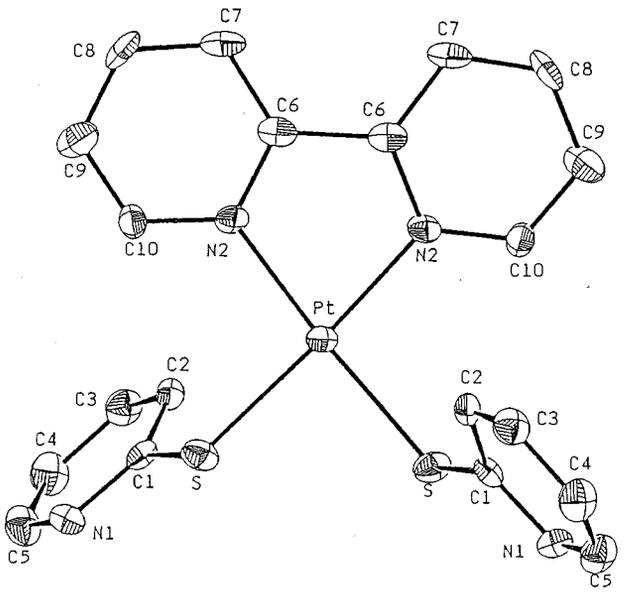

Fig. 1 A perspective view of complex **1** representing the thermal ellipsoids with 30% probabilities.

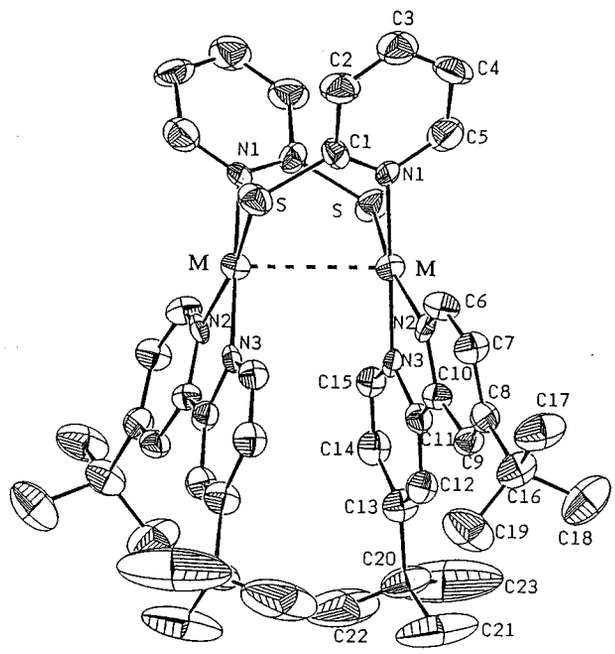

Fig. 2 A perspective view of complexes **3** (M = Pt) and **4** (M = Pd) representing the thermal ellipsoids with 30% probabilities.

298 K. All the data reduction and structural refinement for the above complexes were performed using the NRCC-SDP-VAX package.[11] Intensity data for **8** were collected on a Rigaku AFC7R diffractometer with graphite-monochromated Mo-Kα radiation using the ω–2θ scan mode. Refinement was by full-matrix least squares using the TEXSAN crystallographic software package.[12] The structures were solved by the Patterson method and refined by least-squares cycles. The data were corrected for ψ-scan absorption. Details of crystal parameters, data collection, and structure refinement are given in Table 1. Selected bond distances and bond angles are summarized in Table 2.

CCDC reference number 186/1305.

Results and discussion

The synthesis and photoluminescence properties of mononuclear [Pt(diimine)(dithiolate)] complexes have been extensively studied by Eisenberg and co-workers[6] and others.[13–15] This class of complexes show low energy LLCT [$RS^-(p_\pi)\rightarrow$ diimine(π^*)] absorption bands with λ_{max} ranging from 434 to 679 nm, and photoluminescence at 590–795 nm in solution at room temperature. Eisenberg and co-workers[6] showed that the LLCT absorption and emission energies can be tuned through the electron-donating and -accepting properties of substituents on the diimine and thiolate ligands.

To extend previous studies, we set about the preparation and study of the spectroscopic properties of dinuclear platinum(II) thiolates containing aromatic diimine ligands. The complexes studied in this work were prepared by treating the thiolate ligands with the appropriate platinum(II) precursor. All the newly prepared complexes are stable in solid form for days and some of their structures were characterized by X-ray crystallography. For the purpose of comparison a related dinuclear palladium(II) thiolate complex which is isostructural to **3** has also been prepared.

Crystal structures

The structure of complexes **1**, **3**, **4**, **5**, **6** and **8** are shown in Figs. 1–5, respectively. Similar to the structure of (4,4′-di-*tert*-butylbipyridine)bis(pyridine-4-thiolato)platinum(II), the two pyridine-2-thiolate ligands in **1** are in an *anti* configuration and nearly perpendicular to the PtN_2S_2 planes (dihedral angle = 75.0°). This orientation may explain the lack of close intermolecular $Pt^{II}\cdots Pt^{II}$ and/or ligand–ligand contact in the crystal lattice. The Pt–S and Pt–N(2) bond distances are 2.300(3) and 2.069(9) Å, respectively.

The complex cation **3** has an approximate two-fold axis perpendicular to the $Pt^{II}\cdots Pt^{II}$ axis. The dihedral angle of 16.4° between the two PtN_2S_2 planes suggests that the two dtbpy moieties move away from each other; presumably this is due to the steric hindrance of the *tert*-butyl substituents. The $Pt^{II}\cdots Pt^{II}$ distance of 2.917(2) Å is shorter than the values of 3.083(1) Å in $[Pt_2(en)_2(C_5H_4NS)_2]Cl_2$ (en = ethylenediamine),[16] 3.101(1) Å in $[Pt_2(en)_2(4\text{-}MeC_5H_3NS)_2]Cl_2$[16] and 3.270(1) Å in $[\{Pt(C^\wedge N^\wedge N)\}_2(dppm)][ClO_4]_2$ [C^N^N = 6-phenyl-2,2′-bipyridine; dppm = bis(diphenylphosphino)methane].[3c] It is, however, comparable to the value of 2.925(1) Å in $K_4[Pt_2(P_2O_5H_2)_4]$.[17] This short intramolecular distance could lead to weak $Pt^{II}\cdots Pt^{II}$ and/or ligand–ligand interactions. The Pt–S bond distance is 2.289(5) Å, and the Pt–N (NS) and Pt–N_{ave} (dtbpy) distances are 1.988(14) and 2.002(13) Å, respectively. Complex **4** is isomorphous to **3**. The intramolecular metal–metal distances are very similar for **3** and **4**. The $Pd^{II}\cdots Pd^{II}$ distance of 2.891(4) Å in the Pd_2 dimer is significantly longer than those of 2.677(1) Å in $[Pd_2(NS)_4]$[18] and of 2.745(1) Å in $[Pd_2(bttz)_4]$ (bttz = 1,3-benzothiazole-2-thiolate),[19] but still shorter than the sum of the van der Waals radii for Pd atoms (≈3.26 Å),[20] which implies the presence of weak $Pd^{II}\cdots Pd^{II}$ interactions.

In the crystal lattice of complex **5** the cations exist in pairs with close intermolecular $Pt^{II}\cdots Pt^{II}$ and/or ligand–ligand contacts. A similar structure $[Pt(terpy)(HET)]NO_3$ (HET = SCH_2CH_2OH) had previously been reported by Lippard and co-workers.[21] As shown in Fig. 3, the head-to-tail stacking of the two cations is related by a centre of inversion. The $Pt^{II}\cdots Pt^{II}$ distance of 3.377(1) Å compares well with the related value of 3.329(1) Å in $[Pt(terpy)Cl][CF_3SO_3]$,[3b] and is shorter than those of 3.45 Å in the red form of $[Pt(bpy)Cl_2]$[22] and 3.572(1) Å in $[Pt(terpy)(HET)]NO_3$.[22] The stacking arrangement of the two cations shown in Fig. 3 also reveals weak interactions between two terpy ligands as evidenced by the interplanar separation of *ca.* 3.44 Å (N1···N3′ and N1′···N3′). There is no close intermolecular contact between two interacting pairs of the complex cations. Presumably, this is due to the steric hindrance imposed by the pyridine-2-thiolate ligands that are approximately perpendicular to the PtN_3S planes (dihedral angle = 73.3°). Unlike **5**, **6** exists as a discrete molecule in the

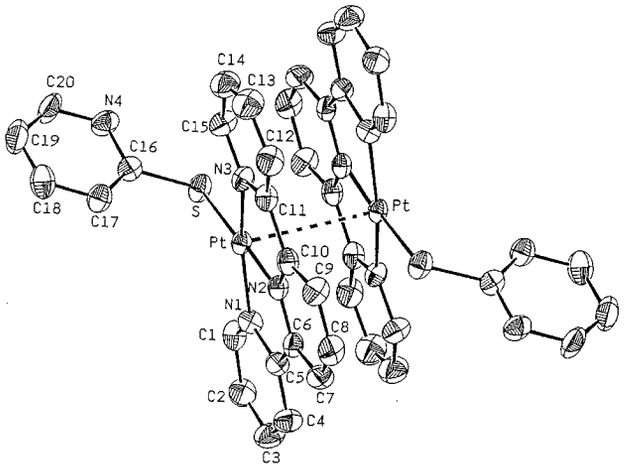

Fig. 3 A perspective view showing the interacting pair of the complex cation in the crystal lattice of **5** representing the thermal ellipsoids with 30% probabilities.

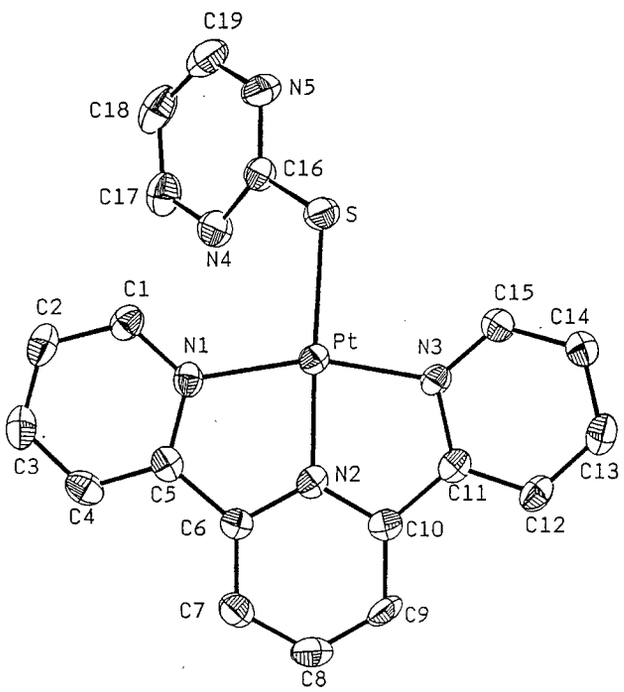

Fig. 4 A perspective view of the complex cation of **6** representing the thermal ellipsoids with 30% probabilities.

crystal lattice. The Pt–S and Pt–N bond distances of **5** and **6** are similar.

As depicted in Fig. 5, complex **8** has two non-interacting $[PtN_3S]$ units with intramolecular $Pt^{II}\cdots Pt^{II}$ separation 4.501(1) Å. The two $Pt^{II}N_3S$ co-ordination planes are in a *syn* configuration with a dihedral angle of 14.0° between them. The closest intermolecular $Pt^{II}\cdots Pt^{II}$ contacts are 3.908(1) and 4.941(1) Å suggesting no intermolecular interaction. Indeed, the structure of **8** is similar to that of $[\{Pt(terpy)\}_2(SCH_2CH_2NH_2)_2][BF_4]_4$[23] which has two nearly parallel Pt^{II}–terpy planes with a separation of 4.420 Å.

Spectroscopic and photophysical properties

UV-VIS Absorption spectra. Spectroscopic and photophysical data are listed in Table 3, and some representative spectra are shown in Fig. 6(a)–6(d). In general, complexes **1**, **2** and **3** show intense absorption bands at 250–360 nm and with broad absorption extending from 400 to 600 nm. For **1** and **2** the absorption maxima of the low-energy bands are at 480 and 465 nm, respectively. Complex **3** shows a similar weak absorption with λ_{max} at 488 nm [Fig. 6(b)], and an intense band at

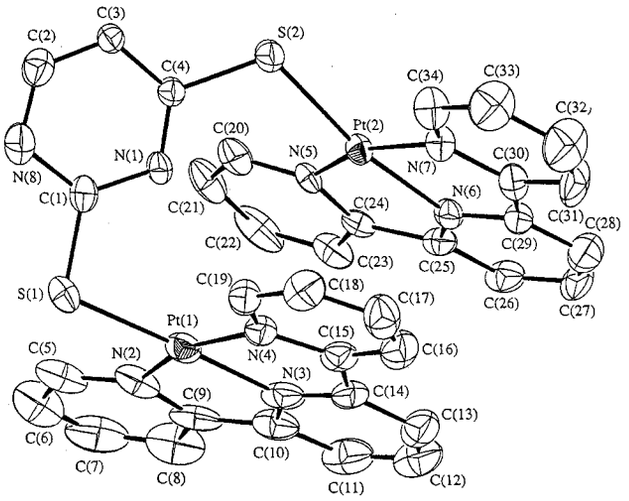

Fig. 5 A perspective view of the complex cation of **8** representing the thermal ellipsoids with 30% probabilities.

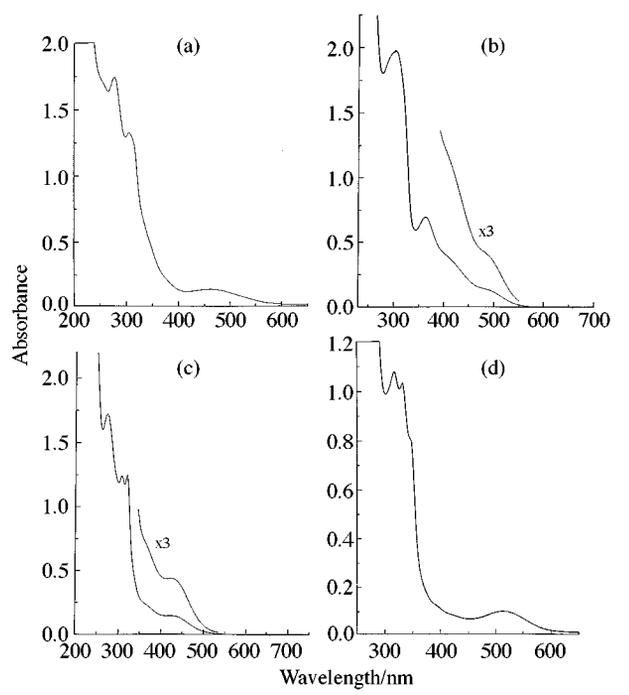

Fig. 6 Absorption spectra at room temperature of (a) complex **2** in dichloromethane (1.0×10^{-4} M), (b) **3** (M = Pt) in dichloromethane (6.8×10^{-5} M), (c) **4** (M = Pd) in dichloromethane (5.2×10^{-5} M) and (d) **8** in acetonitrile (5.65×10^{-5} M).

362 nm which is conspicuously absent in the spectra of **1** and **2**. The absorption spectrum of **4** [Fig. 6(c)] is similar to that of **2** except that the absorptivities in the visible region are much lower in the former case. Complexes **5**, **6**, **7** and **8**, which contain a terpyridine ligand, show intense vibronic structured absorptions at 300–350 nm and broad absorption at 400–600 nm with maxima at 520, 482, 510 and 515 nm, respectively.

Based on the similarity to those of diimines and thiolates, the high-energy absorption bands of the platinum(II) diimine complexes **1**, **2** and **3** can be attributed to intraligand transitions. A detailed assignment of such bands, however, is prevented by band overlapping. Those low-energy absorptions ranging from 400 to 600 nm are unlikely to be due to intraligand transitions since these absorptions are absent from the spectra of $[Pt(dtbpy)Cl_2]$ and 'free' ligands. Indeed, these absorptions are similar to the LLCT transitions of 546 nm of $[Pt(bpy)(MeC_6H_3S_2\text{-}3,4)]$[5a] and of 435–563 nm of [Pt(dtbpy)(dithiolate)].[6] Notably, the low-energy absorptions of the complexes studied in this work are in a similar spectral region, irrespective

Table 1 Crystallographic data

	1	**3**·CH_3OH	**4**·CH_3OH	**5**	**6**	**8**
Formula	$C_{20}H_{16}N_4PtS_2$	$C_{47}H_{60}Cl_2N_6O_9Pt_2S_2$	$C_{47}H_{60}Cl_2N_6O_9Pd_2S_2$	$C_{40}H_{30}Cl_2N_8O_8Pt_2S_2$	$C_{19}H_{14}ClN_5O_4PtS$	$C_{34}H_{24}Cl_2N_8O_8Pt_2S_2$
M	571.58	1346.17	1168.80	1275.92	638.95	1197.82
Space group	*Pbcn*	*Pbcn*	*Pbcn*	$P2_1/c$	$P2_1/n$	$P\bar{1}$
Crystal system	orthorhombic	orthorhombic	orthorhombic	monoclinic	monoclinic	triclinic
a/Å	20.847(4)	12.651(4)	12.596(4)	9.827(2)	8.483(3)	12.640(4)
b/Å	9.306(2)	35.480(9)	35.564(8)	21.302(3)	12.761(3)	13.023(3)
c/Å	9.364(2)	12.299(3)	12.316(4)	10.694(1)	18.225(3)	13.092(2)
α/°						88.33(2)
β/°				112.93(2)	91.42(2)	67.59(2)
γ/°						66.59(2)
V/Å^3	1817(1)	5520(3)	5517(3)	2062(1)	1973(1)	1809(1)
Z	4	4	4	2	4	2
F(000)	1090	2668	2452	1218	1218	1140
μ/cm^{-1}	80.55	114.76	74.25	72.4	74.62	80.21
D_c/g cm^{-3}	2.09	1.62	1.41	2.06	2.15	2.20
T/K	298	298	298	298	298	298
No. parameters used	124	309	309	281	281	505
$2\theta_{max}$/°	55	120	120	50	50	43
No. unique reflections	2077	4092	3934	3636	3465	4140
No. reflections with $I > 2\sigma(I)$	1194	2150	1551	2589	2400	2993 [$I > 3\sigma(I)$]
R, R'	0.031, 0.032	0.056, 0.057	0.082, 0.088	0.030, 0.029	0.035, 0.035	0.028, 0.026
Goodness of fit	2.71	2.18	2.14	1.53	1.24	1.47

of the presence or absence of metal–metal and/or ligand–ligand interactions. For example, complexes **1** and **3** show similar absorption bands at 480 and 488 nm respectively, but the latter is a dinuclear platinum(II) complex with intramolecular metal–metal/ligand–ligand interactions. The apparent blue shift in the low energy absorption maxima from **3** (488 nm) to **4** (421 nm) indicates that the LLCT transitions in the platinum(II) thiolate complexes may have some MLCT [5d (Pt) $\longrightarrow$ π* (diimine)] character.

For complexes **5**, **6**, **7** and **8** the vibronic-structured absorption band at 300–350 nm with vibrational progressions ranging from 1300 to 1400 cm^{-1} is characteristic of intraligand transition of terpyridine ligands. Similar absorption bands have been reported for $[Pt(terpy)X]^+$ (X = halide, N_3^- or SCN^-)[3b] and $[Pt_2(terpy)_2(Gua)][ClO_4]_3$ (Gua = guanine anion).[3a,b] However, their low-energy broad absorptions at 400 to 650 nm are absent for $[Pt(terpy)X]^+$,[3b] but are comparable in energy to that of the MMLCT band [d_{σ^*}(Pt–Pt) $\longrightarrow$ π*(terpy)] of $[Pt_2(terpy)_2(Gua)][ClO_4]_3$ at 483 nm;[3a,b] the latter complex has intramolecular $Pt^{II}\cdots Pt^{II}$ separations of 3.090(1) and 3.071(1) Å, but complexes **6** and **7** have no intramolecular close contacts. Although complex **5** exists as a dimeric structure with a $Pt^{II}\cdots Pt^{II}$ distance of 3.377(1) Å in the solid state, it does not undergo any significant aggregation at concentrations up to 10^{-3} mol dm^{-3}; the relation between the absorbance and complex concentration follows Beer's law. Thus for the terpyridine complexes studied in this work we assign the low-energy absorption bands at 400–600 nm to LLCT transitions. The following experiments have been undertaken to support this LLCT assignment.

The solvent dependence of the low-energy absorption band of complex **2** which has a good solubility in organic solvents has been studied. The absorption maximum was found to blue shift with increasing solvent polarity [solvent, λ_{max}/nm (ε/dm^3 mol^{-1} cm^{-1})]: acetonitrile, 438 (2629); dimethylformamide, 448 (1955); acetone, 459 (2090); dichloromethane, 465 (1880); chloroform, 471 (2155); tetrahydrofuran, 483 (1800). For comparison, the related $[Pt(dtbpy)Cl_2]$ does not show a similar solvatochromic absorption band. The solvent dependence of the LLCT transitions of platinum(II) thiolates containing aromatic diimine ligands has previously been rationalized by the change in dipole moments between the ground and excited states.[5a,6]

The LLCT absorption energy is also dependent on the electron-donating and -accepting properties of substituents on the thiolate and diimine (terpyridine) ligands and the substituent effect can be depicted by Scheme 2. The π*- and π-orbital

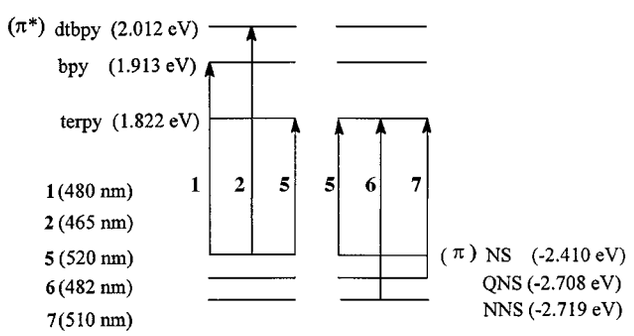

Scheme 2 The LLCT transitions for some related complexes showing substituent effects.

energies of the thiolate and diimine (terpyridine) ligands used in this work are taken from Hartree–Fock self-consistent field (HF-SCF) calculation results. Complexes **1**, **2** and **5** have the same thiolate ligand, but their diimine ligands are different with LUMO energies in the order **2** > **1** > **5**, which matches with that of the low-energy absorption maxima of these three complexes. On the other hand, complexes **5**–**7** have the same terpyridine ligand and their absorption maxima decrease in energy in parallel with the increase in HOMO energy of the thiolate ligands. This supports a LLCT assignment.

Emission spectra

All the platinum complexes show photoluminescence in the solid state and/or in solution at room temperature, whereas the palladium complex **4** is non-emissive. As representatives, the solution emission spectra of **3** and **8** are shown in Fig. 7. The emission data are listed in Table 3. The dinuclear Pt^{II}_2 complex **3** shows a solid state emission maximum at 606 nm at room temperature, which is at a higher energy than that of **1** at 645 nm, even though the latter has no close intermolecular contact in the crystal lattice, whereas the former has an intramolecular $Pt^{II}\cdots Pt^{II}$ contact of 2.917(2) Å. It is interesting that the emission maxima of the mononuclear complexes **5**–**7** are at energies even lower than that of the dinuclear complex **3**. Upon

Table 2 Selected bond distances (Å) and angles (°) for complexes **1**, **3**–**6** and **8**

1			
Pt–S	2.300(3)	Pt–N(2)	2.069(9)
S–Pt–S	88.3(1)	S–Pt–N(2)	96.1(3)
S–Pt–N(2)	175.6(3)		
3			
Pt···Pt	2.917(2)	Pt–S	2.289(5)
Pt–N(1)	1.988(14)	Pt–N(2)	2.023(12)
Pt–N(3)	1.980(13)		
N(1)–Pt–N(2)	96.6(6)	N(1)–Pt–N(3)	176.4(5)
N(2)–Pt–N(3)	80.0(5)	S–Pt–N(1)	88.8(4)
S–Pt–N(2)	168.1(4)	S–Pt–N(3)	94.8(4)
4			
Pd···Pd	2.891(4)	Pd–S	2.275(4)
Pd–N(1)	2.04(2)	Pd–N(2)	2.03(2)
Pd–N(3)	2.009(18)		
N(1)–Pd–N(2)	97.0(7)	N(1)–Pd–N(3)	175.1(7)
N(2)–Pd–N(3)	78.2(7)	S–Pd–N(1)	89.8(5)
S–Pd–N(2)	166.6(6)	S–Pd–N(3)	95.1(5)
5			
Pt···Pt(a)	3.377(1)	Pt–S	2.299(2)
Pt–N(1)	2.034(6)	Pt–N(2)	1.947(6)
Pt–N(3)	2.023(6)		
N(1)–Pt–N(2)	81.5(3)	N(1)–Pt–N(3)	161.9(3)
N(2)–Pt–N(3)	80.3(3)	S–Pt–N(1)	98.8(2)
S–Pt–N(2)	179.2(2)	S–Pt–N(3)	99.3(2)
6			
Pt–S	2.307(3)	Pt–N(1)	2.035(7)
Pt–N(2)	1.936(7)	Pt–N(3)	2.034(7)
N(1)–Pt–N(2)	80.1(3)	N(1)–Pt–N(3)	161.2(3)
N(2)–Pt–N(3)	81.1(3)	S–Pt–N(1)	102.6(2)
S–Pt–N(2)	177.3(2)	S–Pt–N(3)	96.2(2)
8			
Pt(1)–S(1)	2.303(3)	Pt(2)–S(2)	2.295(3)
Pt(1)–N(2)	2.04(1)	Pt(1)–N(3)	1.98(1)
Pt(1)–N(4)	2.03(1)	Pt(2)–N(5)	2.027(9)
Pt(2)–N(6)	1.964(8)	Pt(2)–N(7)	2.013(9)
S(1)–Pt(1)–N(2)	97.1(4)	S(1)–Pt(1)–N(3)	178.5(4)
S(1)–Pt(1)–N(4)	101.2(3)	N(2)–Pt(1)–N(3)	81.5(6)
N(2)–Pt(1)–N(4)	161.7(5)	N(4)–Pt(1)–N(4)	80.2(5)
S(2)–Pt(2)–N(5)	103.3(3)	S(2)–Pt(2)–N(6)	169.9(2)
S(2)–Pt(2)–N(7)	95.8(3)	N(5)–Pt(2)–N(6)	80.4(4)
N(5)–Pt(2)–N(7)	160.8(4)	N(6)–Pt(2)–N(7)	80.3(4)

cooling to 77 K the solid state emissions of the complexes increase in intensity, but with no notable shift in energy. With reference to previous works on [Pt(bpy)($MeC_6H_3S_2$-3,4)] and [Pt(dtbpy)(dithiolate)] complexes,[6] we assign the emissions described above to the LLCT (thiolate→diimine charge-transfer) excited states.

The complex $[Pt_2(terpy)_2(Gua)][ClO_4]_3$,[3a,b] can be regarded as a model for probing the photoluminescence arising from metal–metal and/or ligand–ligand interaction of two interacting platinum(II) terpyridine units. In solution this complex emits at 620 nm, which is at a similar energy to that of the excimeric emission of the [Pt(diimine)$(CN)_2$] solids (diimine = dtbpy, 565 nm;[4c] 4,7-diphenyl-1,10-phenanthroline, 630 nm[5b]). Another related complex is [Pt(C^N^N-dpp)(CH_3CN)]ClO_4 (C^N^N-dpp = 2,9-diphenyl-1,10-phenanthroline),[4a] which has an intermolecular $Pt^{II}\cdots Pt^{II}$ contact of 3.372(1) Å and its solid state emission is at 680 nm. These low-energy emissions of $[Pt_2(terpy)_2(Gua)][ClO_4]_3$, [Pt(diimine)$(CN)_2$] and [Pt(C^N^N-dpp)$(CH_3CN)$]$ClO_4$ solids come from the MMLCT [d_{σ^*}(Pt–Pt) ⟶ π*(terpy)/(bpy)] excited states.

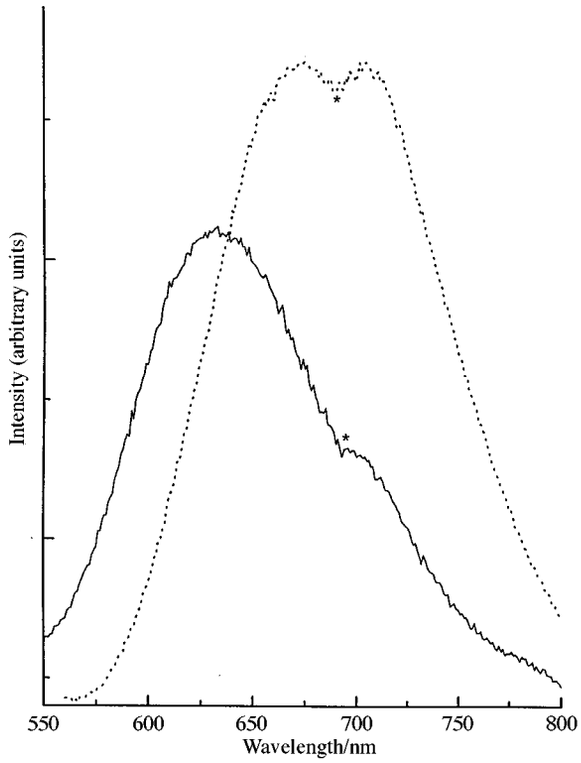

Fig. 7 Emission spectra of complexes **3** (——) and **8** (– – – –) in dichloromethane and acetonitrile respectively at room temperature. Excitation at 300–400 nm (* artifact).

The emission of the platinum(II) thiolate complexes studied here are at 603–710 nm, comparable in energy to those of the MMLCT emission of the complexes described above.[4a] This fact may account for the absence of excimeric emission in platinum(II) thiolates containing aromatic diimines. For those platinum(II) thiolates of diimines with intra- and/or intermolecular $Pt^{II}\cdots Pt^{II}$ and/or ligand–ligand contacts larger than 2.9 Å, such as the ones studied in this work, the LLCT excited states may be lower in energy than the MMLCT one (Scheme 1). In monomeric platinum(II) thiolates LLCT is the lowest excited state. Since excimeric emission comes from the interaction between the ground and excited state through metal–metal bonding interactions,[4,5b] a low-energy Pt^{II} ⟶ π*(diimine) transition is a prerequisite. This is because effective metal–metal bonding interactions would require at least one metal atom in an open-shell electronic configuration. The Pt^{II} ⟶ π*(diimine) excited state has the platinum atom in a formal oxidation state +3 with a 17-electron configuration, and this facilitates the metal–metal bonding interaction.

Conclusion

A series of platinum(II) thiolates with bipyridine and terpyridine ligands have been prepared and some of their structures determined by X-ray crystallography. The shift in absorption energy with changes in the electronic properties of the substituents on the diimine and thiolate ligands confirms the assignment of a LLCT excited state.

The $Pt^{II}\cdots Pt^{II}$ and/or ligand–ligand interactions are not primarily responsible for the low-energy absorptions and emissions, even in the case of complex **3**, which has a shorter $Pt^{II}\cdots Pt^{II}$ contact than those in $[Pt_2(terpy)_2(Gua)][ClO_4]_3$, [Pt(C^N^N-dpp)$(CH_3CN)$]$ClO_4$, and some linear-chain platinum(II) diimine complexes that are known to display low-energy [d_{σ^*}(Pt–Pt) ⟶ π*(bpy or terpy)] excited states. We

Table 3 Spectroscopic and photophysical properties

Complexes	M · · · M/Å	Medium (T/K)	λ_{abs}/nm (ε/dm^3 mol^{-1} cm^{-1})	Emission λ_{max}/nm	Lifetime τ/μs	Quantum yield
1	—	CH_2Cl_2 (298)	275 (12 720); 304 (sh) (8680); 480 (620)	Non-emissive		
		Solid (298)		645	0.30	
		Solid (77)		645		
2		CH_2Cl_2 (298)	278 (17 600); 307 (13 300); 465 (1880)	Non-emissive		
		Solid (298)		635	0.10	
		Solid (77)		618		
3	2.917(2)	CH_2Cl_2 (298)	302 (29 311); 362 (10 292); 408 (sh) (5752); 488 (sh) (1976)	603	0.68	[a] 4.30×10^{-4}
		Solid (298)		606	0.32	
		Solid (77)		610		
4	2.891(4)	CH_2Cl_2 (298)	272 (34 059); 306 (24 049); 318 (23 846); 360 (sh) (4518); 421 (2517)	Non-emissive		
		Solid (298)		Non-emissive		
5	3.377(1)	CH_3CN (298)	314 (10 510); 330 (10 560); 346 (9490); 520 (640)	Non-emissive		
		Solid (298)		640	0.16	
		Solid (77)		640		
6	—	CH_3CN (298)	313 (8910); 328 (8670); 345 (8480); 482 (750)	650	0.34	[b] 6.10×10^{-4}
		Solid (298)		650	0.29	
		Solid (77)		650		
7		CH_3CN (298)	315 (7700); 330 (8600); 346 (8580); 510 (570)	708	0.30	[c] 1.80×10^{-4}
		Solid (298)		710	0.25	
		Solid (77)		665		
8	3.908(1)	CH_3CN (298)	316 (19 030); 331 (18 120); 346 (14 010)	702	0.22	[d] 5.61×10^{-4}
	4.501(1)	Solid (298)		660	0.30	
		Solid (77)		670		

Complex concentration: [a] 6.76×10^{-5}; [b] 1.64×10^{-4}; [c] 2.03×10^{-4}; [d] 6.77×10^{-5} M.

suggest that the LLCT excited states occur at even lower energy than those of the MMLCT ones.

Acknowledgements

We acknowledge supports from the University of Hong Kong and the Hong Kong Research Grants Council.

References

1 J. A. Bailey, V. M. Miskowski and H. B. Gray, *Inorg. Chem.*, 1993, **32**, 369.
2 V. M. Miskowski and V. H. Houlding, *Inorg Chem.*, 1989, **28**, 1529; V. H. Houlding and V. M. Miskowski, *Coord. Chem. Rev.*, 1991, **111**, 145; V. M. Miskowski and V. H. Houlding, *Inorg. Chem.*, 1991, **30**, 4446.
3 (*a*) H.-K. Yip, C.-M. Che, Z.-Y. Zhou and T. C.-W. Mak, *J. Chem. Soc., Chem. Commun.*, 1992, 1369; (*b*) H.-K. Yip, L.-K. Cheng, K.-K. Cheung and C.-M. Che, *J. Chem. Soc., Dalton Trans.*, 1993, 2933; (*c*) T.-C. Cheung, K.-K. Cheung, S.-M. Peng and C.-M. Che, *J. Chem. Soc., Dalton Trans.*, 1996, 1645.
4 (*a*) C.-W. Chan, T.-F. Lai, C.-M. Che and S.-M. Peng, *J. Am. Chem. Soc.*, 1993, **115**, 11245; (*b*) C.-W. Chan, L.-K. Cheng and C.-M. Che, *Coord. Chem. Rev.*, 1994, **132**, 87; (*c*) K.-T. Wan, C.-M. Che and K.-C. Cho, *J. Chem. Soc., Dalton Trans.*, 1991, 1077.
5 A. Vogler and H. Kunkely, *J. Am. Chem. Soc.*, (*a*) 1981, **103**, 1559; (*b*) 1990, **112**, 5625.
6 W. Paw, R. J. Lachicotte and R. Eisenberg, *Inorg. Chem.*, 1998, **37**, 4141; S. D. Cummings and R. Eisenberg, *J. Am. Chem. Soc.*, 1996, **118**, 1949; *Inorg. Chem.*, 1995, **34**, 2007; J. M. Bevilacqua and R. Eisenberg, *Inorg. Chem.*, 1994, **33**, 2913; J. M. Bevilacqua, J. A. Zuleta and R. Eisenberg, *Inorg. Chem.*, 1993, **32**, 3689; J. A. Zuleta, M. S. Burberry and R. Eisenberg, *Coord. Chem. Rev.*, 1990, **97**, 47.
7 K. A. Truesdell and G. A. Crosby, *J. Am. Chem. Soc.*, 1985, **107**, 1787; G. A. Crosby, R. G. Highland and K. A. Truesdell, *Coord. Chem. Rev.*, 1985, **64**, 41.
8 G. M. Bager and W. H. F. Sasse, *J. Chem. Soc.*, 1956, 616.
9 M. Howe-Grant and S. J. Lippard, *Inorg. Synth.*, 1980, **20**, 102.
10 F. G. Mann and H. R. Watson, *J. Chem. Soc.*, 1958, 2772.
11 E. J. Gabe, Y. LePage, J. P. Charland and P. S. White, *J. Appl. Crystallogr.*, 1989, **22**, 384.
12 TEXSAN, Crystal Structure Analysis Package, Molecular Structure Corporation, Houston, TX, 1985 and 1992.
13 J. A. Weinstein, N. N. Zheligovskaya, M. Y. Mel'nikov and F. Hartl, *J. Chem. Soc., Dalton Trans.*, 1998, 2459.
14 W. B. Connick and H. B. Gray, *J. Am. Chem. Soc.*, 1997, **119**, 11620.
15 K. Base and M. W. Grinstaff, *Inorg. Chem.*, 1998, **37**, 1432.
16 J. Umakoshi, I. Kinoshita, Y. Fukui-Yasuba, K. Matsumoto, S. Ooi, H. Nakai and M. Shiro, *J. Chem. Soc., Dalton Trans.*, 1989, 815.
17 D. M. Roundhill, H. B. Gray and C.-M. Che, *Acc. Chem. Res.*, 1989, **22**, 55.
18 K. Umakoshi, A. Ichimura, I. Kinoshita and S. Ooi, *Inorg. Chem.*, 1990, **29**, 4005.
19 M. Kubiak, *Acta Crystallogr., Sect. C*, 1987, **41**, 1288.
20 A. Bondi, *J. Phys. Chem.*, 1964, **68**, 441.
21 K. W. Jennette, J. T. Gill, J. A. Sadownick and S. J. Lippard, *J. Am. Chem. Soc.*, 1976, **98**, 6159.
22 R. S. Osborn and D. Rogers, *J. Chem. Soc., Dalton Trans.*, 1974, 1002.
23 J. C. Dewan, S. J. Lippard and W. R. Bauer, *J. Am. Chem. Soc.*, 1980, **102**, 858.

Paper 8/09287G